MOFs as Photoactuators

How to cite:
International Edition: doi.org/10.1002/anie.202218052
German Edition: doi.org/10.1002/ange.202218052

Substrate-Bound Diarylethene-Based Anisotropic Metal–Organic Framework Films as Photoactuators with a Directed Response

*Yunzhe Jiang[+], Yidong Liu[+], Sylvain Grosjean, Volodymyr Bon, Patrick Hodapp, Anemar Bruno Kanj, Stefan Kaskel, Stefan Bräse, Christof Wöll, and Lars Heinke**

Abstract: Molecular machines and responsive materials open a plethora of new opportunities in nanotechnology. We present an oriented crystalline array of diarylethene (DAE)-based photoactuators, arranged in a way to yield an anisotropic response. The DAE units are assembled, together with a secondary linker, into a monolithic surface-mounted metal–organic framework (SURMOF) film. By Infrared (IR) and UV/Vis spectroscopy as well as by synchrotron X-ray diffraction, we show that the light-induced extension changes of the molecular DAE linkers multiply to yield mesoscopic and anisotropic length changes. Due to the special architecture and substrate-bonding of the SURMOF, these length changes are transferred to the macroscopic scale, leading to the bending of a cantilever and performing work. This research shows the potential of assembling light-powered molecules into SURMOFs to yield photoactuators with a directed response, presenting a path to advanced actuators.

Introduction

Artificial molecular machines and actuators have the potential to revolutionize several fields in medicine, (micro-) robotics and the internet of things.[1] Inspired by the muscles of animals, actuators change their extension as a response to external stimuli and perform mechanical work. Using light as fuel to stimulate motion allows for a clean, fast and accurate powering. In this way, numerous light-powered actuators have been realized.[2] These efforts are typically based on artificial light-responsive materials, which reversibly change their properties upon interaction with photons.[1a] Often, photoresponsive materials are based on molecules that reversibly and repeatedly isomerize between two or more forms as response to the absorption of light of different wavelengths.[3] Due to their favorable photophysical properties, azobenzene, spiropyran and diarylethene have been extensively explored.[3b,4]

So far, most molecular photoresponsive actuators were based on polymers, where the subunits are randomly oriented.[5] Moreover, molecular crystals of the photoswitches were presented, where the molecular units are held together by non-covalent interactions.[6] In this way, several photon-driven nanodevices could be realized, including micro-particle transportation, shape-deformation and a walker fueled by light.[6a,d,7] The direction of the response in such materials is often controlled by mesoscopic structuring or by the direction of the light irradiation (and light shielding). Although these demonstrations are impressive, two shortcomings should be overcome to enable further advanced applications, e.g. in micro-robotics: The device integration needs to be improved and the responsive material must be rigidly attached, ideally by chemical bonds, to other materials. The photoactuating material should be prepared on different substrates in a controlled manner, providing a determined anisotropic response.

Metal–organic frameworks (MOFs) are materials with a regular framework structure composed of metal nodes connected by organic linker molecules.[8] MOF structures can be tailored to specific needs by the choice of their

[*] Y. Jiang,[+] Y. Liu,[+] Dr. A. B. Kanj, Prof. Dr. C. Wöll, Dr. L. Heinke
Institute of Functional Interfaces (IFG), Karlsruhe Institute of Technology (KIT)
Hermann-von-Helmholtz-Platz 1, 76344 Eggenstein-Leopoldshafen (Germany)
E-mail: Lars.Heinke@kit.edu

Dr. S. Grosjean, Dr. P. Hodapp, Prof. Dr. S. Bräse
Soft Matter Synthesis Laboratory, Institute for Biological Interfaces 3 (IBG 3), Karlsruhe Institute of Technology (KIT)
Hermann-von-Helmholtz-Platz 1, 76344 Eggenstein-Leopoldshafen (Germany)

Dr. V. Bon, Prof. Dr. S. Kaskel
Inorganic Chemistry I, Technische Universität Dresden
Bergstraße 66, 01069 Dresden (Germany)

Prof. Dr. S. Bräse
Institute of Organic Chemistry (IOC), Karlsruhe Institute of Technology (KIT)
Fritz-Haber-Weg 6, 76131 Karlsruhe (Germany)
and
Institute of Biological and Chemical Systems - Functional Molecular Systems (IBCS-FMS), Karlsruhe Institute of Technology (KIT)
Hermann-von-Helmholtz-Platz 1, 76344 Eggenstein-Leopoldshafen (Germany)

[+] These authors contributed equally to this work.

components, for example resulting in variable pore sizes and functionalities.[9] While most MOF materials are made in the form of powders, homogeneous films can also be prepared.[10] The incorporation of photoresponsive molecules allows the control of various properties of the MOF material by light.[11] In this way, photoswitches like azobenzene and spiropyran have been integrated into MOFs to control the adsorption, diffusion and membrane separation as well as the ionic and electron conduction properties by light.[12] However, the assembly of photoactive linkers into MOFs to yield photoactive materials is not straightforward, e.g. switching of the linkers might be blocked by interactions with the MOF lattice,[13] or the photoisomerization even leads to a collapse of the MOF structure.[14] Besides, MOF-types using only one type of linkers yield an isotropic response, thus, a directional motion requires, for example, polarized light or localized light irradiation and light shielding.

A promising candidate for a photoswitchable linker is diarylethene (DAE). Irradiation with light can induce a transformation between the two DAE isomers (open and closed form) via bond formation/cleavage between two heterocyclic thiophenes.[6f,15] The isomerization process happens without large-scale rotation and flipping, a fact which is crucial with regard to the integration in the crystalline MOF backbone.[6f] In addition, DAE compounds typically exhibit a high quantum yield, a short response time, a large fatigue resistance, and a highly adjustable excitation wavelength,[6f,16] all very favorable parameters for photoactuators. The relaxation time of the closed-form-DAE to the thermodynamically stable open-form-DAE is very slow and the DAE molecules are considered p-type photoswitches (which isomerize photochemically reversible but thermally irreversible). Several works have reported on MOFs with DAE either in the linker backbone or as side groups.[12d,17] In a few cases,[17g,h] the change of the lattice parameters upon DAE photoisomerization has been reported. However, all these previous efforts have been limited to powders, a form of MOF materials not well suited for device applications, in particular as photoactuators. Recently, free-standing MOF crystals which bend upon light irradiation, caused by [2+2] cycloaddition and based on azobenzene, have been presented.[18] To date, a MOF photoactuator performing mechanical work, e.g. in form of bending a substrate, has not been reported.

Here, we realized DAE-based, highly anisotropic MOF thin films rigidly attached to a substrate by coordination bonds sufficiently strong enough to transfer mechanical forces. The pyridine-substituted DAE-molecules were assembled, together with a non-photoactive secondary linker and a paddle-wheel metal node, into a crystalline array. It yields a MOF thin film with a pillared-layer structure, where the DAE acts as pillar (Figure 1). The DAE-MOF film was grown directly on the substrate in a layer-by-layer fashion, resulting in surface-mounted MOFs (SURMOFs).[19] The SURMOFs were chemically grafted to the substrate, in this case via Cu-OH-coordination bonds to a thiol-based self-assembled monolayer on a flat gold substrate. The SURMOFs can be grown with controlled orientation,[20] resulting in the formation of a highly anisotropic DAE-photoactuator array. The reversible ring-opening-closing photoisomerization in the DAE-SURMOF was explored and quantified by IR and UV/Vis spectroscopy. Employing synchrotron X-ray diffraction, the change of the lattice parameter was determined to be about 1 %. In order to demonstrate macroscopic effects, the DAE-SURMOFs were deposited on a flexible gold-coated mica substrate. The bending of these cantilevers could be determined readily and allowed to quantitatively study the photoactuation as well as the light-induced forces and work. This is the first report of the use of photoswitchable molecules as the backbone in a SURMOF or any other MOF thin film for the realization of substrate bending and mechanical work.

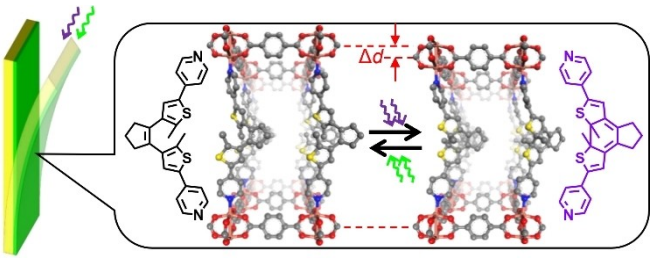

Figure 1. Sketch of the DAE-SURMOF, i.e. SURMOF films of type $Cu_2(BDC)_2$(DAE-Py), with the photoswitchable diarylethene molecules (DAE-Py) as pillar-linkers. During the photoisomerization, the length of the DAE linker molecule and, thus, of the MOF lattice changes by Δd. The open form, which is reached upon green-light irradiation ($\lambda = 530$ nm), is shown on the left-hand side. The closed form, reached upon UV-light irradiation ($\lambda = 365$ nm), is shown on the right-hand side.

Results and Discussion

The synthesis of DAE-SURMOF was performed in a layer-by-layer fashion[19d] by subsequently exposing the substrate to the solutions of the MOF components, which were copper acetate as metal nodes as well as BDC (1,4-benzenedicarboxylic acid = terephthalic acid) and DAE-Py (see Figure 1) as linkers. The DAE-SURMOF has a pillared-layer structure of type $Cu_2(BDC)_2$(DAE-Py). More information on the DAE-Py[21] and SURMOF synthesis is given in the Supporting Information. Before the SURMOF synthesis, the substrate was functionalized with a thiol-based self-assembled monolayer (SAM). For the X-ray diffraction and spectroscopy, the substrate, which was a gold-coated silicon wafer, was functionalized with a 11-mercapto-1-undecanol SAM, resulting in a OH-terminated surface.

The X-ray diffractograms (XRD, Figure 2) show that the prepared DAE-SURMOF films were crystalline with the targeted structure.[22] Moreover, the out-of-plane XRD shows only peaks of (00*n*) type, indicating the oriented growth of the MOF film. The high crystalline orientation was also verified by the in-plane XRD patterns containing exclusively reflections perpendicular to the [001] direction. This indicates that the DAE-SURMOF was grown in a crystalline and highly oriented fashion, where the Cu-paddle

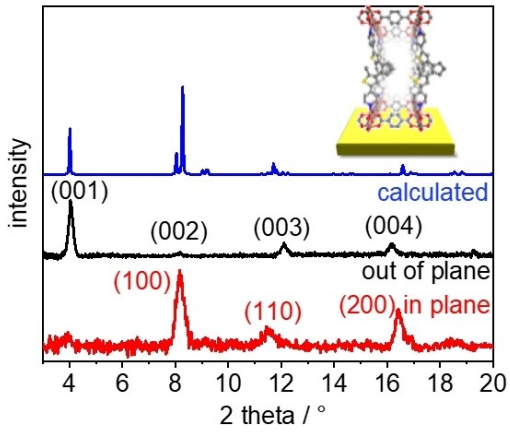

Figure 2. Out-of-plane XRD (black), in-plane XRD (red) of the DAE-SURMOF and the calculated XRD of the targeted structure (blue). The inset shows the MOF structure on the substrate. The experimentally observed diffraction peaks are labelled.

wheels and BDC linker molecules form layers parallel to the substrate and DAE-Py molecules stand perpendicular as pillars (see inset in Figure 2). The SEM images of the sample (Figure S1, Supporting Information) show that the DAE-SURMOF films represent a dense 200 nm thick polycrystalline layer.

The photoisomerization of the DAE-SURMOF was explored by UV/Vis spectroscopy, Figure 3a. For clearly recognizing small changes in the spectra, their differences are shown in Figure 3b. Upon irradiation with UV light and with visible light, a small band at approximately 630 nm evolves and vanishes, respectively. For comparison, the UV/Vis spectra of the DAE linker in solution are shown in Figure S3. The spectra of the SURMOF are in line with the spectra of the DAE linker in solution and in agreement with the literature,[6f,15] indicating the reversible UV-light-induced ring-closing and the visible-light-induced ring-opening of the DAE moiety. The reversibility was explored by a series of repeated switching by irradiation with different light exposure times, Figure 3c. The data show that a maximum of the switching effect was realized for an irradiation time of 5 min for UV light and approximately 9 min for visible light. Longer irradiation time does not increase the photoisomerization yield. The data also indicate that the pristine spectrum was not fully recovered, this means a small photobleaching effect after a few isomerization cycles can be observed. Further UV/Vis experiments (Figure S4) show that various visible light wavelengths can trigger the transition from the closed-form to the open-form, where green light shows the fastest photoisomerization. It also shows that the switching yield decreases significantly over 10 irradiation cycles.

For quantifying the switching yield and the photostationary state, infrared reflection absorption spectroscopy (IRRAS) was employed (Figure 3d). In the spectra, the strongest bands at 1640 cm^{-1} and 1395 cm^{-1} can be attributed to the asymmetric stretching mode of COO^- and symmetric stretching mode of C–O,[23] indicating the formation of the DAE-SURMOF. Upon UV irradiation, the spectrum was almost unaltered, with the exception that new bands appear at 770 cm^{-1} and 700 cm^{-1}. At the same time, the bands at 850 cm^{-1}, 830 cm^{-1} and 720 cm^{-1} decreased, see Figure S5. These changes, which were attributed to the vibrational changes of the methyl group, indicate the photoisomerization of the DAE moieties. The band at approximately 720 cm^{-1} is not overlapped by other vibrations and can be used to quantify the DAE photoisomerization yield, see inset in Figure 3d. Initially, the DAE-SURMOF was in the thermodynamically stable, 100 %-ring-open state. Upon UV-light, the band intensity decreased to 40.2 %, indicating a photostationary state with 40 % ring-open and 60 % ring-closed DAE moieties in the DAE-SURMOF sample. Upon visible light irradiation, a spectrum which is essentially identical to the pristine spectrum was obtained, indicating the reversibility of the photoisomerization.

The structural changes in the DAE-SURMOF structure as a result of the ring-opening and -closing was explored by synchrotron X-ray diffraction where the sample was irradiated *in situ*, see also Supporting Information. The DAE-SURMOF was grown in [001] direction, which is the direction with the DAE-pillar in the MOF backbone, see the sketch in Figure 2. The experimental data are shown in Figure 4 and S6. Figure 3a shows the (001) peaks of the pristine sample and upon UV- and visible-light irradiation. The peak position was determined by a Gaussian fit and the lattice distance for four photoswitching cycles was calculated (Figure 4b). The data of higher order reflections are shown in Figure S6. Upon UV light irradiation ($\lambda = 365$ nm), the peak maximum shifted from 2 theta = 4.062° to 2 theta = 4.088° indicating the linear contraction of the unit cell by 0.64 % in [001] direction. This change of the unit cell volume is obtained under similar conditions as in Figures 3d, where a conversion yield of 60 % was determined. A higher conversion yield would presumably result in a larger change of the average unit cell volume, as determined by XRD.

The reversibility of photoswitching in DAE-SURMOF was proven by visible light ($\lambda = 530$ nm) irradiation, which induces expansion of the structure to the initial state (Figure 4a). Three subsequent irradiation cycles indicate the reversibility of the phenomenon (Figure 4b), however, the amplitude of switching decreased after the first cycle, indicating a bleaching effect of DAE-SURMOF, also supported by the spectroscopy data (above).

The synchrotron XRD data on the light-induced changes of the lattice parameters were reproduced with the data recorded at common state-of-the-art X-ray diffractometers, Figure S7a. In addition, the in-plane XRD data verify the statement that the lattice parameters in the Cu(BDC) layer are not affected by the DAE-photoisomerization. Only the distance between these planes, that is in [001] direction, was affected, see Figure S7b.

For taking advantage of the light-induced changes of the lattice distance in [001] direction, a DAE-SURMOF was grown on a modified substrate under optimized conditions,[20d] so that there were domains with the crystalline [001] direction parallel to the substrate surface. So, the photoinduced changes of the MOF lattice distance along the

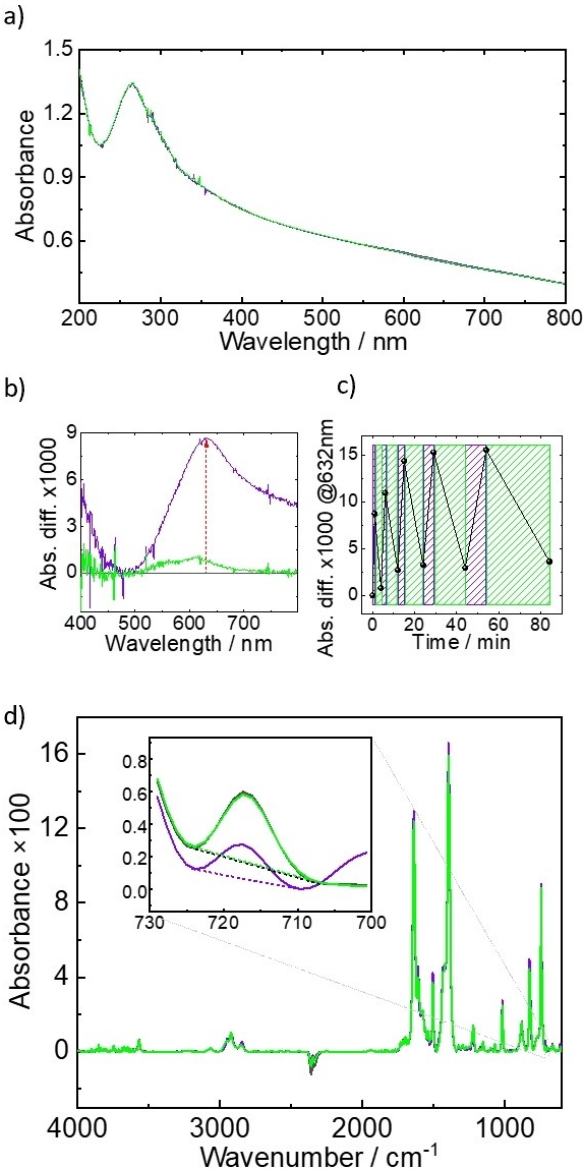

Figure 3. a) UV/Vis spectra of the DAE-SURMOF before (black) and after UV-light ($\lambda = 365$ nm) irradiation (violet) and after green-light ($\lambda = 530$ nm) irradiation (green). b) The differential absorbance spectra of the (very similar) UV/Vis spectra in panel a) with the pristine spectrum as reference. c) The absorbance at 632 nm (band of closed-DAE) of the DAE-SURMOF during 5 irradiation cycles with different irradiation times (right). The irradiation times were 1 min, 2 min, 3 min, 5 min and 10 min, respectively for UV-light and 3 min, 6 min, 9 min, 15 min and 30 min, respectively for visible light. The corresponding spectra are shown in Figure S2. d) IRRA spectra of the DAE-SURMOF before (black) and after UV-light ($\lambda = 365$ nm) irradiation (violet) and after green-light ($\lambda = 530$ nm) irradiation (green). The green and black spectra are virtually identical. The inset shows the zoom-in of the open-DAE vibration for the quantification of the photostationary state.

[001] direction induce a strain into the substrate. The substrate was a gold-coated mica sheet of 40 mm length and 5 mm width. The thickness of the substrate was approximately 2.6 µm, see Figure S8c. The sample was clamped on one side, resulting in a free cantilever with a length of

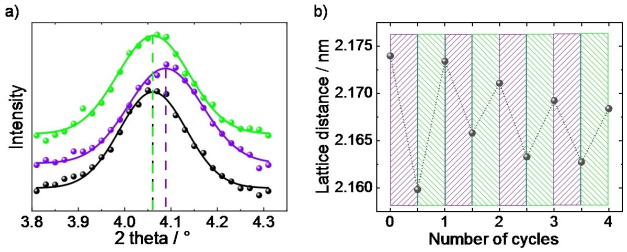

Figure 4. a) Synchrotron out-of-plane XRD of DAE-SURMOF. The pristine sample is shown in black, after UV light ($\lambda = 365$ nm) in violet and after green light ($\lambda = 530$ nm) in green. The lines are the Gaussian fits to the data. b) The lattice distance in [001] direction for four UV/Visible-light-irradiation cycles.

25 mm (Figure 5a, a photo of the setup is shown Figure S9). The sample position, i.e. the deflection of the cantilever was recorded with a high-resolution camera.

The deflection of the sample during the irradiation with UV and green light for 3 cycles is shown in Figure 5b. Without light irradiation, the sample does not change its position. Upon irradiation with UV light, the cantilever deflection gradually increased by approximately 100 µm, corresponding to a bending angle of about 4 mrad (which is $\approx 0.23°$). The sample remains in this position until the irradiation with visible light, which causes the sample deflection to return to its original position. The illumination-induced cantilever deflection was rather stable, in line with the pronounced stability of the ring-closed and -open forms of DAE. The macroscopic cantilever deflection is a direct result of the microscopic photoisomerization of the pillar linkers in the DAE-SURMOF. Upon UV-light irradiation, the SURMOF lattice shrinks, bending the cantilever in the direction of the SURMOF, and vice versa upon green light. The bending of the sample as a result of the UV and green light irradiation is essentially reversible, indicating the stability of the DAE-SURMOF sample. Further, repeatability experiments were performed in Figures 5c and SI12. The data show that the irradiation with UV and green light results in the reversible bending of the cantilever for many cycles. The bending magnitude decreases slightly, i.e. by about 35 % during the course of 13 photoactuation cycles. This is in line with the fatigue found by UV/Vis and XRD experiments, see above.

In calibration experiments, the spring constant of the sample was determined to be 11.2 N mm^{-1}, Figure S10. Thus, the photoinduced changes of the DAE-SURMOF provide a force of 1.12 µN and an energy of 0.112 nJ to the flexible substrate. As a rough estimation, a light-to-work energy efficiency in the order of 10^{-12}–10^{-11} follows. In comparison to other light-powered actuators, which have energy efficiencies typically in the order of 10^{-12}–10^{-7} (see ref. [24] and references in them), the efficiency is rather low, suggesting that the performance of the SURMOF actuators can (and should) be further improved.

For reference, we performed bending experiments with a bare substrate which has a similar spring constant. For this sample, no photoactuation was observed, indicating that the

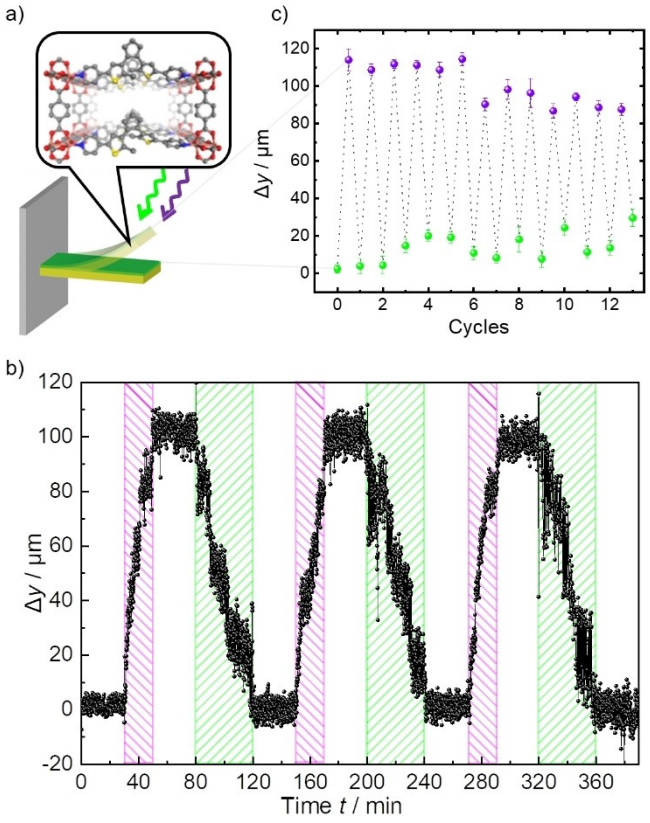

Figure 5. SURMOF-cantilever photoactuation. a) Sketch of the cantilever deflection. The SURMOF is on the bottom-side of the Au@mica cantilever. b) Cantilever deflection of the SURMOF@Au@mica-sample during three UV- and visible-light-irradiation cycles, indicated by the violet and green boxes. The video of the cantilever deflection is provided in the Supporting Information online. The three cycles are essentially identical and the (average) cantilever position for the open- and closed-form DAE-SURMOF are the same (within a deviation of 2 µm). c) The cantilever deflection during the irradiation with UV light (violet) spheres and with green light (green spheres) for 13 irradiation cycles. The transient cantilever deflection data are shown in Figure SI12. (Different samples were used in panel b and c, so the deflection is slightly different.)

bending of the cantilever is caused by the SURMOF grown on top (Figure S11).

The SEM images of the SURMOF grown on the Au@mica substrate (the sample used as photoactuator in Figures 5b) are shown in Figure S8b. It shows that, although the film has a rather rough morphology, all parts of the substrate are covered. The thickness of the monolithic, dense film was approximately 0.5 µm. The in-plane XRD of the SURMOF on the Au@mica-cantilever shows that the sample was grown in mixed orientations (Figure S8a). A detailed inspection of the XRD data of the sample shows that about half of the MOF domains were grown in (100) orientation, this means the [001] direction is parallel to the substrate surface. These domains are able to cause strain on the substrate. Moreover, the MOF domains which are oriented with the [001] direction parallel to the substrate surface have arbitrary in-plane orientations. As a simplified estimation, from these MOF domains, half of them cause strain perpendicular to the cantilever direction (and are not able to bend the cantilever), while the other half can cause strain in the direction of the cantilever, resulting in its bending. In the future, an in-plane orientation of the SURMOF by advanced substrates[25] is envisioned, resulting in an anisotropic strain of the film.

Conclusion

Oriented pillar-layered SURMOF films with photoswitchable diarylethene molecules in the backbone were grown on solid substrates. The DAE-ring-opening and -closing photoisomerization results in a change of the SURMOF-lattice-constant in [001] direction, as explored by *in situ* synchrotron XRD supported by UV/Vis and infrared spectroscopy. The light-powered directed shrinking and expansion of the SURMOF was used to reversibly bend a flexible substrate and to provide forces in the micro-Newton-range and perform work in the nano-Joule-range.

Due to the flexibility of the SURMOF approach, we believe that the photoactuation performance can be further enhanced. For example, different molecular photoactuators including dimethyldihydropyrene (DHP), fulgide and norbornadiene[26] can be incorporated in such oriented substrate-bound crystalline films, potentially allowing a larger directed response. Apart from enlarging the photoactuation magnitude, a major aim will be to enhance the number of reversible cycles and the actuation speed. Moreover, we will focus on optimizing the SURMOF film quality, including the film thickness as well as the orientation of the domains in cantilever direction to enhance the photoactuation performance.[25a] We will particularly focus on the optimization of SURMOF growth conditions, e.g. using machine-learning approaches. In addition, the SURMOF approach facilitates the preparation of structured films[27] with a controlled layering of different responsive layers. This enables the preparation of complex photoresponsive structures. Overall, this SURMOF-based approach offers a further path to realize intelligent, complex and multifunctional materials and actuators.

Acknowledgements

We thank the Volkswagen Foundation, the German Research Foundation (DFG, FOR2433) and the China Scholarship Council (CSC) for financial support. Dr. D. Wallacher, N. Grimm and Dr. D. M. Többens are acknowledged for assistance during *in situ* PXRD measurements at KMC-2 beamline of BESSY II synchrotron. We thank the Helmholtz-Zentrum Berlin für Materialien und Energie for the allocation of synchrotron radiation beamtime at KMC-2 beamline. This research has been funded by the Deutsche Forschungsgemeinschaft (DFG, German Research Foundation) under Germany's Excellence Strategy via the Excellence Cluster "3D Matter Made to Order" (3DMM2O, EXC-2082/1-390761711). Open Access funding enabled and organized by Projekt DEAL.

Conflict of Interest

The authors declare no conflict of interest.

Data Availability Statement

The data that support the findings of this study are available from the corresponding author upon reasonable request.

Keywords: Diarylethene · Metal–Organic Frameworks · Photo-Switching · Photoactuator · Thin Films

[1] a) F. Soto, E. Karshalev, F. Zhang, B. Esteban Fernandez de Avila, A. Nourhani, J. Wang, *Chem. Rev.* **2022**, *122*, 5365–5403; b) I. L. Sokolov, V. R. Cherkasov, A. A. Tregubov, S. R. Buiucli, M. P. Nikitin, *Biochim. Biophys. Acta Gen. Subj.* **2017**, *1861*, 1530–1544; c) N. El-Atab, R. B. Mishra, F. Al-Modaf, L. Joharji, A. A. Alsharif, H. Alamoudi, M. Diaz, N. Qaiser, M. M. Hussain, *Adv. Intell. Syst.* **2020**, *2*, 2000128; d) P. Rothemund, Y. Kim, R. H. Heisser, X. Zhao, R. F. Shepherd, C. Keplinger, *Nat. Mater.* **2021**, *20*, 1582–1587; e) L. Hines, K. Petersen, G. Z. Lum, M. Sitti, *Adv. Mater.* **2017**, *29*, 1603483; f) J. Yunas, B. Mulyanti, I. Hamidah, M. Mohd Said, R. E. Pawinanto, W. A. F. Wan Ali, A. Subandi, A. A. Hamzah, R. Latif, B. Yeop Majlis, *Polymer* **2020**, *12*, 1184.

[2] a) R. Yin, W. Xu, M. Kondo, C.-C. Yen, J.-i. Mamiya, T. Ikeda, Y. Yu, *J. Mater. Chem.* **2009**, *19*, 3141; b) J. Boelke, S. Hecht, *Adv. Opt. Mater.* **2019**, *7*, 1900404; c) L. Wang, Q. Li, *Chem. Soc. Rev.* **2018**, *47*, 1044–1097; d) J. Chen, F. K. Leung, M. C. A. Stuart, T. Kajitani, T. Fukushima, E. van der Giessen, B. L. Feringa, *Nat. Chem.* **2018**, *10*, 132–138.

[3] a) M. M. Russew, S. Hecht, *Adv. Mater.* **2010**, *22*, 3348–3360; b) B. L. Feringa, W. R. Browne, *Molecular Switches*, Wiley, Hoboken, **2011**.

[4] a) A. Goulet-Hanssens, F. Eisenreich, S. Hecht, *Adv. Mater.* **2020**, *32*, 1905966; b) C.-Y. Lai, G. Raj, I. Liepuoniute, M. Chiesa, P. Naumov, *Cryst. Growth Des.* **2017**, *17*, 3306–3312; c) P. Naumov, P. Yu, K. Sakurai, *J. Phys. Chem. A* **2008**, *112*, 5810–5814; d) I. Liepuoniute, P. Commins, D. P. Karothu, S. Schramm, H. Hara, P. Naumov, *Chem. Eur. J.* **2019**, *25*, 373–378; e) Z. L. Pianowski, *Molecular Photoswitches: Chemistry, Properties, and Applications*, Wiley, Hoboken, **2022**.

[5] a) P. F. Luo, S. L. Xiang, C. Li, M. Q. Zhu, *J. Polym. Sci.* **2021**, *59*, 2246–2264; b) A. H. Gelebart, D. Jan Mulder, M. Varga, A. Konya, G. Vantomme, E. W. Meijer, R. L. B. Selinger, D. J. Broer, *Nature* **2017**, *546*, 632–636; c) M. Yamada, M. Kondo, J. Mamiya, Y. Yu, M. Kinoshita, C. J. Barrett, T. Ikeda, *Angew. Chem. Int. Ed.* **2008**, *47*, 4986–4988; *Angew. Chem.* **2008**, *120*, 5064–5066; d) R. Costil, M. Holzheimer, S. Crespi, N. A. Simeth, B. Feringa, *Chem. Rev.* **2021**, *121*, 13213–13237.

[6] a) S. Kobatake, S. Takami, H. Muto, T. Ishikawa, M. Irie, *Nature* **2007**, *446*, 778–781; b) F. Terao, M. Morimoto, M. Irie, *Angew. Chem. Int. Ed.* **2012**, *51*, 901–904; *Angew. Chem.* **2012**, *124*, 925–928; c) D. Kitagawa, S. Kobatake, *Chem. Commun.* **2015**, *51*, 4421–4424; d) R. Nishimura, A. Fujimoto, N. Yasuda, M. Morimoto, T. Nagasaka, H. Sotome, S. Ito, H. Miyasaka, S. Yokojima, S. Nakamura, B. L. Feringa, K. Uchida, *Angew. Chem. Int. Ed.* **2019**, *58*, 13308–13312; *Angew. Chem.* **2019**, *131*, 13442–13446; e) M. Irie, S. Kobatake, M. Horichi, *Science* **2001**, *291*, 1769–1772; f) M. Irie, T. Fukaminato, K. Matsuda, S. Kobatake, *Chem. Rev.* **2014**, *114*, 12174–12277.

[7] H. Zeng, P. Wasylczyk, C. Parmeggiani, D. Martella, M. Burresi, D. S. Wiersma, *Adv. Mater.* **2015**, *27*, 3883–3887.

[8] a) H. C. Zhou, S. Kitagawa, *Chem. Soc. Rev.* **2014**, *43*, 5415–5418; b) H. Furukawa, K. E. Cordova, M. O'Keeffe, O. M. Yaghi, *Science* **2013**, *341*, 1230444.

[9] A. Kirchon, L. Feng, H. F. Drake, E. A. Joseph, H. C. Zhou, *Chem. Soc. Rev.* **2018**, *47*, 8611–8638.

[10] a) I. Stassen, N. C. Burtch, A. A. Talin, P. Falcaro, M. D. Allendorf, R. Ameloot, *Chem. Soc. Rev.* **2017**, *46*, 3853–3853; b) E. Virmani, J. M. Rotter, A. Maehringer, T. von Zons, A. Godt, T. Bein, S. Wuttke, D. D. Medina, *J. Am. Chem. Soc.* **2018**, *140*, 4812–4819; c) I. Stassen, M. Styles, G. Grenci, H. Van Gorp, W. Vanderlinden, S. De Feyter, P. Falcaro, D. De Vos, P. Vereecken, R. Ameloot, *Nat. Mater.* **2016**, *15*, 304–310.

[11] a) R. Haldar, L. Heinke, C. Wöll, *Adv. Mater.* **2020**, *32*, 1905227; b) Y. Z. Jiang, L. Heinke, *Langmuir* **2021**, *37*, 2–15; c) F. Bigdeli, C. T. Lollar, A. Morsali, H.-C. Zhou, *Angew. Chem. Int. Ed.* **2020**, *59*, 4652–4669; *Angew. Chem.* **2020**, *132*, 4680–4699; d) A. Modrow, D. Zargarani, R. Herges, N. Stock, *Dalton Trans.* **2011**, *40*, 4217–4222; e) S. Krause, J. D. Evans, V. Bon, S. Crespi, W. Danowski, W. R. Browne, S. Ehrling, F. Walenszus, D. Wallacher, N. Grimm, D. M. Többens, M. S. Weiss, S. Kaskel, B. L. Feringa, *Nat. Commun.* **2022**, *13*, 1951.

[12] a) J. Park, L. B. Sun, Y. P. Chen, Z. Perry, H. C. Zhou, *Angew. Chem. Int. Ed.* **2014**, *53*, 5842–5846; *Angew. Chem.* **2014**, *126*, 5952–5956; b) L. Heinke, *J. Phys. D* **2017**, *50*, 193004; c) S. Garg, H. Schwartz, M. Kozlowska, A. B. Kanj, K. Muller, W. Wenzel, U. Ruschewitz, L. Heinke, *Angew. Chem. Int. Ed.* **2019**, *58*, 1193–1197; *Angew. Chem.* **2019**, *131*, 1205–1210; d) C. B. Fan, Z. Q. Liu, L. L. Gong, A. M. Zheng, L. Zhang, C. S. Yan, H. Q. Wu, X. F. Feng, F. Luo, *Chem. Commun.* **2017**, *53*, 763–766; e) Z. Wang, A. Knebel, S. Grosjean, D. Wagner, S. Bräse, C. Wöll, J. Caro, L. Heinke, *Nat. Commun.* **2016**, *7*, 13872; f) K. Müller, J. Helfferich, F. Zhao, R. Verma, A. B. Kanj, V. Meded, D. Bleger, W. Wenzel, L. Heinke, *Adv. Mater.* **2018**, *30*, 1706551.

[13] Z. Wang, L. Heinke, J. Jelic, M. Cakici, M. Dommaschk, R. J. Maurer, H. Oberhofer, S. Grosjean, R. Herges, S. Bräse, K. Reuter, C. Wöll, *Phys. Chem. Chem. Phys.* **2015**, *17*, 14582–14587.

[14] a) A. Schaate, S. Duhnen, G. Platz, S. Lilienthal, A. M. Schneider, P. Behrens, *Eur. J. Inorg. Chem.* **2012**, 790–796; b) C. C. Epley, K. L. Roth, S. Lin, S. R. Ahrenholtz, T. Z. Grove, A. J. Morris, *Dalton Trans.* **2017**, *46*, 4917–4922.

[15] M. Irie, *Chem. Rev.* **2000**, *100*, 1685–1716.

[16] a) H. Tian, S. Yang, *Chem. Soc. Rev.* **2004**, *33*, 85–97; b) M. Herder, B. M. Schmidt, L. Grubert, M. Pätzel, J. Schwarz, S. Hecht, *J. Am. Chem. Soc.* **2015**, *137*, 2738–2747.

[17] a) E. A. Dolgopolova, V. A. Galitskiy, C. R. Martin, H. N. Gregory, B. J. Yarbrough, A. M. Rice, A. A. Berseneva, O. A. Ejegbavwo, K. S. Stephenson, P. Kittikhunnatham, S. G. Karakalos, M. D. Smith, A. B. Greytak, S. Garashchuk, N. B. Shustova, *J. Am. Chem. Soc.* **2019**, *141*, 5350–5358; b) F. Luo, C. B. Fan, M. B. Luo, X. L. Wu, Y. Zhu, S. Z. Pu, W. Y. Xu, G. C. Guo, *Angew. Chem. Int. Ed.* **2014**, *53*, 9298–9301; *Angew. Chem.* **2014**, *126*, 9452–9455; c) J. Park, D. Feng, S. Yuan, H. C. Zhou, *Angew. Chem. Int. Ed.* **2015**, *54*, 430–435; *Angew. Chem.* **2015**, *127*, 440–445; d) I. M. Walton, J. M. Cox, C. A. Benson, D. G. Patel, Y.-S. Chen, J. B. Benedict, *New J. Chem.* **2016**, *40*, 101–106; e) D. G. Patel, I. M. Walton, J. M. Cox, C. J. Gleason, D. R. Butzer, J. B. Benedict, *Chem. Commun.* **2014**, *50*, 2653–2656; f) I. M. Walton, J. M. Cox, J. A. Coppin, C. M. Linderman, D. G. Patel, J. B. Benedict, *Chem. Commun.* **2013**, *49*, 8012–8014; g) Y. Zheng, H. Sato, P. Wu, H. J. Jeon, R. Matsuda, S. Kitagawa, *Nat. Commun.* **2017**, *8*, 100; h) V. I. Nikolayenko, S. A. Herbert, L. J. Barbour, *Chem. Commun.* **2017**, *53*, 11142–11145.

[18] a) J.-s. Geng, L. Mei, Y.-y. Liang, L.-y. Yuan, J.-p. Yu, K.-q. Hu, L.-h. Yuan, W. Feng, Z.-f. Chai, W.-q. Shi, *Nat. Commun.* **2022**, *13*, 2030; b) Z. H. Pang, L. Dang, L. Yang, F. Luo, *J. Solid State Chem.* **2019**, *277*, 182–186; c) Y.-X. Shi, W.-H. Zhang, B. F. Abrahams, P. Braunstein, J.-P. Lang, *Angew. Chem. Int. Ed.* **2019**, *58*, 9453–9458; *Angew. Chem.* **2019**, *131*, 9553–9558.

[19] a) O. Shekhah, H. Wang, T. Strunskus, P. Cyganik, D. Zacher, R. Fischer, C. Wöll, *Langmuir* **2007**, *23*, 7440–7442; b) L. Heinke, C. Wöll, *Adv. Mater.* **2019**, *31*, 1806324; c) O. Shekhah, *Materials* **2010**, *3*, 1302–1315; d) O. Shekhah, H. Wang, S. Kowarik, F. Schreiber, M. Paulus, M. Tolan, C. Sternemann, F. Evers, D. Zacher, R. A. Fischer, C. Wöll, *J. Am. Chem. Soc.* **2007**, *129*, 15118–15119.

[20] a) J. Liu, O. Shekhah, X. Stammer, H. K. Arslan, B. Liu, B. Schüpbach, A. Terfort, C. Wöll, *Materials* **2012**, *5*, 1581–1592; b) D. Zacher, K. Yusenko, A. Bétard, S. Henke, M. Molon, T. Ladnorg, O. Shekhah, B. Schüpbach, T. de los Arcos, M. Krasnopolski, M. Meilikhov, J. Winter, A. Terfort, C. Wöll, R. A. Fischer, *Chem. Eur. J.* **2011**, *17*, 1448–1455; c) J.-L. Zhuang, M. Kind, C. M. Grytz, F. Farr, M. Diefenbach, S. Tussupbayev, M. C. Holthausen, A. Terfort, *J. Am. Chem. Soc.* **2015**, *137*, 8237–8243; d) Q. Li, J. Gies, X.-J. Yu, Y. Gu, A. Terfort, M. Kind, *Chem. Eur. J.* **2020**, *26*, 5185–5189.

[21] S. Grosjean, P. Hodapp, Chemotion Repository, pp. https://dx.doi.org/10.14272/collection/PH2_2023-01-27.

[22] Deposition Numbers 2238146 (for the open-DAE form) and 2238145 (for the closed-DAE form) contain the supplementary crystallographic data for this paper. These data are provided free of charge by the joint Cambridge Crystallographic Data Centre and Fachinformationszentrum Karlsruhe Access Structures service.

[23] L. Panahi, M. R. Naimi-Jamal, J. Mokhtari, A. Morsali, *Microporous Mesoporous Mater.* **2017**, *244*, 208–217.

[24] a) H. Okamura, *Optomechatronic Actuators, Manipulation, and Systems Control, Vol. 6374*, SPIE, Bellingham, **2006**, p. 637401; b) J. Mahmoud Halabi, E. Ahmed, S. Sofela, P. Naumov, *Proc. Natl. Acad. Sci. USA* **2021**, *118*, e2020604118.

[25] a) P. Falcaro, K. Okada, T. Hara, K. Ikigaki, Y. Tokudome, A. W. Thornton, A. J. Hill, T. Williams, C. Doonan, M. Takahashi, *Nat. Mater.* **2017**, *16*, 342–348; b) S. Klokic, D. Naumenko, B. Marmiroli, F. Carraro, M. Linares-Moreau, S. Dal Zilio, G. Birarda, R. Kargl, P. Falcaro, H. Amenitsch, *Chem. Sci.* **2022**, *13*, 11869–11877.

[26] a) J. Volarić, W. Szymanski, N. A. Simeth, B. L. Feringa, *Chem. Soc. Rev.* **2021**, *50*, 12377–12449; b) P. Liesfeld, Y. Garmshausen, S. Budzak, J. Becker, A. Dallmann, D. Jacquemin, S. Hecht, *Angew. Chem. Int. Ed.* **2020**, *59*, 19352–19358; *Angew. Chem.* **2020**, *132*, 19517–19523; c) C. Eichler, A. Razkova, F. Muller, H. Kopacka, H. Huppertz, T. S. Hofer, H. A. Schwartz, *Chem. Mater.* **2021**, *33*, 3757–3766.

[27] a) K. Ikigaki, K. Okada, Y. Tokudome, T. Toyao, P. Falcaro, C. J. Doonan, M. Takahashi, *Angew. Chem. Int. Ed.* **2019**, *58*, 6886–6890; *Angew. Chem.* **2019**, *131*, 6960–6964; b) O. Shekhah, J. Liu, R. A. Fischer, C. Wöll, *Chem. Soc. Rev.* **2011**, *40*, 1081–1106; c) L. Heinke, M. Cakici, M. Dommaschk, S. Grosjean, R. Herges, S. Bräse, C. Wöll, *ACS Nano* **2014**, *8*, 1463–1467.

Manuscript received: December 7, 2022
Accepted manuscript online: February 20, 2023
Version of record online: ■■, ■■

Research Articles

MOFs as Photoactuators

Y. Jiang, Y. Liu, S. Grosjean, V. Bon, P. Hodapp, A. B. Kanj, S. Kaskel, S. Bräse, C. Wöll, L. Heinke* **e202218052**

Substrate-Bound Diarylethene-Based Anisotropic Metal–Organic Framework Films as Photoactuators with a Directed Response

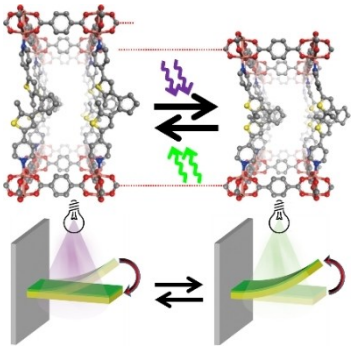

An oriented crystalline array of diarylethene (DAE)-based photoactuators is presented. The DAE units are assembled in a surface-mounted metal–organic framework (SURMOF) film. The light-induced length changes of the DAE linkers multiply to anisotropic mesoscopic length changes. Due to the architecture and substrate-bonding of the SURMOF, these length changes are transferred to the macroscopic scale, here, bending a cantilever and performing work.